

A linear-time algorithm for the geodesic center of a simple polygon

Hee-Kap Ahn^{*3}, Luis Barba^{1,2}, Prosenjit Bose¹, Jean-Lou de Carufel¹, Matias Korman^{4,5}, and Eunjin Oh³

¹ School of Computer Science, Carleton University, Ottawa, Canada.

`jit@scs.carleton.ca, jdecaruf@cg.scs.carleton.ca`

² Département d'Informatique, Université Libre de Bruxelles, Brussels, Belgium.

`lbarbafl@ulb.ac.be`

³ Department of Computer Science and Engineering, POSTECH,

77 Cheongam-Ro, Nam-Gu, Pohang, Gyeongbuk, Korea.

`{heekap, jin9082}@postech.ac.kr`

⁴ National Institute of Informatics (NII), Tokyo, Japan.

`korman@nii.ac.jp`

⁵ JST, ERATO, Kawarabayashi Large Graph Project.

Abstract

Given two points in a simple polygon P of n vertices, its geodesic distance is the length of the shortest path that connects them among all paths that stay within P . The geodesic center of P is the unique point in P that minimizes the largest geodesic distance to all other points of P . In 1989, Pollack, Sharir and Rote [Disc. & Comput. Geom. 89] showed an $O(n \log n)$ -time algorithm that computes the geodesic center of P . Since then, a longstanding question has been whether this running time can be improved (explicitly posed by Mitchell [Handbook of Computational Geometry, 2000]). In this paper we affirmatively answer this question and present a linear time algorithm to solve this problem.

1 Introduction

Let P be a simple polygon with n vertices. Given two points x, y in P , the *geodesic path* $\pi(x, y)$ is the shortest-path contained in P connecting x with y . If the straight-line segment connecting x with y is contained in P , then $\pi(x, y)$ is a straight-line segment. Otherwise, $\pi(x, y)$ is a polygonal chain whose vertices (other than its endpoints) are reflex vertices of P . We refer the reader to [19] for more information on geodesic paths.

The *geodesic distance* between x and y , denoted by $|\pi(x, y)|$, is the sum of the Euclidean lengths of each segment in $\pi(x, y)$. Throughout this paper, when referring to the distance between two points in P , we refer to the geodesic distance between them. Given a point $x \in P$, a (geodesic) *farthest neighbor* of x , is a point $f_P(x)$ (or simply $f(x)$) of P whose geodesic distance to x is maximized. To ease the description, we assume that each vertex of P has a unique farthest neighbor. We can make this *general position* assumption using simulation of simplicity [9].

Let $F_P(x)$ be the function that, for each $x \in P$, maps to the distance to a farthest neighbor of x (i.e., $F_P(x) = |\pi(x, f(x))|$). A point $c_P \in P$ that minimizes $F_P(x)$ is called the *geodesic center* of P . Similarly, a point $s \in P$ that maximizes $F_P(x)$ (together with its farthest neighbor) is called a *geodesic diametral pair* and their distance is known as

* The work by H.-K. Ahn and E. Oh was supported by the NRF grant 2011-0030044 (SRC-GAIA) funded by the Korea government (MSIP).



licensed under Creative Commons License CC-BY



Leibniz International Proceedings in Informatics

LIPICs Schloss Dagstuhl – Leibniz-Zentrum für Informatik, Dagstuhl Publishing, Germany

the *geodesic diameter*. Asano and Toussaint [3] showed that the geodesic center is unique (whereas it is easy to see that several geodesic diametral pairs may exist).

In this paper, we show how to compute the geodesic center of P in $O(n)$ time.

1.1 Previous Work

Since the early 1980s the problem of computing the geodesic center (and its counterpart, the geodesic diameter) has received a lot of attention from the computational geometry community. Chazelle [7] gave the first algorithm for computing the geodesic diameter (which runs in $O(n^2)$ time using linear space). Afterwards, Suri [24] reduced it to $O(n \log n)$ -time without increasing the space constraints. Finally, Hershberger and Suri [13] presented a fast matrix search technique, one application of which is a linear-time algorithm for computing the diameter.

The first algorithm for computing the geodesic center was given by Asano and Toussaint [3], and runs in $O(n^4 \log n)$ -time. In 1989, Pollack, Sharir, and Rote [22] improved it to $O(n \log n)$ time. Since then, it has been an open problem whether the geodesic center can be computed in linear time (indeed, this problem was explicitly posed by Mitchell [19, Chapter 27]).

Several other variations of these two problems have been considered. Indeed, the same problem has been studied under different metrics. Namely, the L_1 geodesic distance [6], the link distance [23, 14, 8] (where we look for the path with the minimum possible number of bends or *links*), or even rectilinear link distance [20, 21] (a variation of the link distance in which only isothetic segments are allowed). The diameter and center of a simple polygon for both the L_1 and rectilinear link metrics can be computed in linear time (whereas $O(n \log n)$ time is needed for the link distance).

Another natural extension is the computation of the diameter and center in polygonal domains (i.e., polygons with one or more holes). Polynomial time algorithms are known for both the diameter [4] and center [5], although the running times are significantly larger (i.e., $O(n^{7.73})$ and $O(n^{12+\varepsilon})$, respectively).

1.2 Outline

In order to compute the geodesic center, Pollack *et al.* [22] introduce a linear time *chord-oracle*. Given a chord C that splits P into two sub-polygons, the oracle determines which sub-polygon contains c_P . Combining this operation with an efficient search on a triangulation of P , Pollack *et al.* narrow the search of c_P within a triangle (and find the center using optimization techniques). Their approach however, does not allow them to reduce the complexity of the problem in each iteration, and hence it runs in $\Theta(n \log n)$ time.

The general approach of our algorithm described in Section 6 is similar: partition P into $O(1)$ cells, use an oracle to determine which cell contains c_P , and recurse within the cell. Our approach differs however in two important aspects that allows us to speed-up the algorithm. First, we do not use the chords of a triangulation of P to partition the problem into cells. We use instead a cutting of a suitable set of chords. Secondly, we compute a set Φ of $O(n)$ functions, each defined in a triangular domain contained in P , such that their upper envelope, $\phi(x)$, coincides with $F_P(x)$. Thus, we can “ignore” the polygon P and focus only on finding the minimum of the function $\phi(x)$.

The search itself uses ε -nets and cutting techniques, which certify that both the size of the cell containing c_P and the number of functions of Φ defined in it decrease by a constant fraction (and thus leads to an overall linear time algorithm). This search has however two stopping conditions, (1) reach a subproblem of constant size, or (2) find a convex trapezoid

containing c_P . In the latter case, we show that $\phi(x)$ is a convex function when restricted to this convex trapezoid. Thus, finding its minimum becomes an optimization problem that we solve in Section 7 using cuttings in \mathbb{R}^3 .

The key of this approach lies in the computation of the functions of Φ and their triangular domains. Each function $g(x)$ of Φ is defined in a triangular domain \triangle contained in P and is associated to a particular vertex w of P . Intuitively speaking, $g(x)$ maps points in \triangle to their (geodesic) distance to w . We guarantee that, for each point $x \in P$, there is one function g defined in a triangle containing x , such that $g(x) = F_P(x)$. To compute these triangles and their corresponding functions, we proceed as follows.

In Section 3, we use the matrix search technique introduced by Hershberger and Suri [13] to decompose the boundary of P , denoted by ∂P , into connected edge disjoint chains. Each chain is defined by either (1) a consecutive list of vertices that have the same farthest neighbor v (we say that v is *marked* if it has such a chain associated to it), or (2) an edge whose endpoints have different farthest neighbors (such edge is called a *transition edge*).

In Section 4, we consider each transition edge ab of ∂P independently and compute its *hourglass*. Intuitively, the hourglass of ab , H_{ab} , is the region of P between two chains, the edge ab and the chain of ∂P that contains the farthest neighbors of all points in ab . Inspired by a result of Suri [24], we show that the sum of the complexities of each hourglass defined on a transition edge is $O(n)$. In addition, we provide a new technique to compute all these hourglasses in linear time.

In Section 5 we show how to compute the functions in Φ and their respective triangles. We distinguish two cases: (1) Inside each hourglass H_{ab} of a transition edge, we use a technique introduced by Aronov et al. [2] that uses the shortest-path trees of a and b in H_{ab} to decompose H_{ab} into $O(|H_{ab}|)$ triangles with their respective functions (for more information on shortest-path trees refer to [10]). (2) For each marked vertex v we compute triangles that encode the distance from v . Moreover, we guarantee that these triangles cover every point of P whose farthest neighbor is v . Overall, we compute the $O(n)$ functions of Φ in linear time.

2 Hourglasses and Funnels

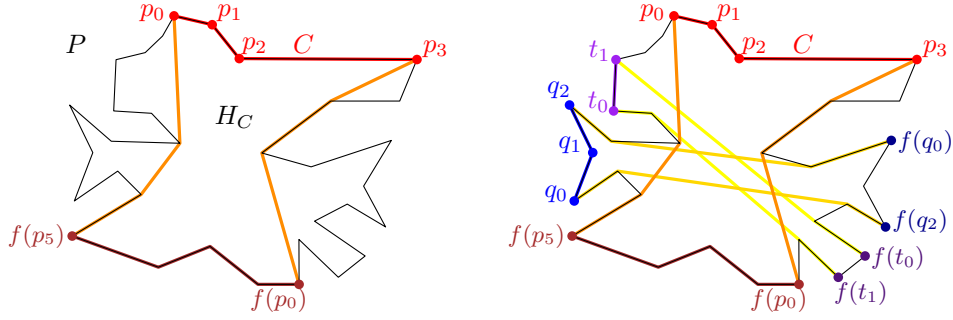
In this section, we introduce the main tools that are going to be used by the algorithm. Some of the results presented in this section have been shown before in different papers. For most of them, we present proof sketches.

2.1 Hourglasses

Given two points x and y on ∂P , let $\partial P(x, y)$ be the polygonal chain that starts at x and follows the boundary of P clockwise until reaching y .

For any polygonal chain $C = \partial P(p_0, p_1, \dots, p_k)$, the *hourglass* of C , denoted by H_C , is the simple polygon contained in P bounded by C , $\pi(p_k, f(p_0))$, $\partial P(f(p_0), f(p_k))$ and $\pi(f(p_k), p_0)$; see Figure 1. We call C and $\partial P(f(p_0), f(p_k))$ the *top* and *bottom* chains of H_C , respectively, while $\pi(p_k, f(p_0))$ and $\pi(f(p_k), p_0)$ are referred to as the *walls* of H_C .

We say that the hourglass H_C is *open* if its walls are vertex disjoint. We say C is a *transition chain* if $f(p_0) \neq f(p_k)$ and neither $f(p_0)$ nor $f(p_k)$ are interior vertices of C . In particular, if an edge ab of ∂P is a transition chain, we say that it is a *transition edge* (see Figure 1).



■ **Figure 1** Given two edge disjoint transition chains, their hourglasses are open and the bottom chains of their hourglasses are also edge disjoint. Moreover, these bottom chains appear in the same cyclic order as the top chains along ∂P .

129 ► **Lemma 1.** [Rephrase of Lemma 3.1.3 of [2]] If C is a transition chain of ∂P , then the
 130 hourglass H_C is an open hourglass.

131 Note that by Lemma 1, the hourglass of each transition chain is open. In the remainder
 132 of the paper, all the hourglasses considered are defined by a transition chain, i.e., they are
 133 open and their top and bottom chains are edge disjoint.

134 The following lemma is depicted in Figure 1 and is a direct consequence of the Ordering
 135 Lemma proved by Aronov et al. [2, Corollary 2.7.4].

136 ► **Lemma 2.** Let C_1, C_2, C_3 be three edge disjoint transition chains of ∂P that appear in this
 137 order when traversing clockwise the boundary of P . Then, the bottom chains of H_{C_1}, H_{C_2} and
 138 H_{C_3} are also edge disjoint and appear in this order when traversing clockwise the boundary
 139 of P .

140 Let γ be a geodesic path joining two points on the boundary of P . We say that γ separates
 141 two points x_1 and x_2 of ∂P if the points of $X = \{x_1, x_2\}$ and the endpoints of γ alternate
 142 along the boundary of P (x_1 and x_2 could coincide with the endpoints of γ in degenerate
 143 cases). We say that a geodesic γ separates an hourglass H if it separates the points of its
 144 top chain from those of its bottom chain.

145 ► **Lemma 3.** Let C_1, \dots, C_r be edge disjoint transition chains of ∂P . Then, there is a set
 146 of $t = O(1)$ geodesic paths $\gamma_1, \dots, \gamma_t$ with endpoints on ∂P such that for each $1 \leq i \leq r$ there
 147 exists $1 \leq j \leq t$ such that γ_j separates H_{C_i} . Moreover, this set can be computed in $O(n)$
 148 time.

149 **Proof.** Aronov et al. showed that there exist four vertices v_1, \dots, v_4 of P and geodesic paths
 150 $\pi(v_1, v_2), \pi(v_2, v_3), \pi(v_3, v_4)$ such that for any point $x \in \partial P$, one of these paths separates x
 151 from $f(x)$ [2, Lemma 2.7.6]. Moreover, they show how to compute this set in $O(n)$ time.

152 Let $\Gamma = \{\pi(v_i, v_j) : 1 \leq i < j \leq 4\}$ and note that v_1, \dots, v_4 split the boundary of P into
 153 at most four connected components. If a chain C_i is completely contained in one of these
 154 components, then one path of Γ separates the top and bottom chain of H_{C_i} . Otherwise,
 155 some vertex v_j is an interior vertex of C_i . However, because the chains C_1, \dots, C_r are edge
 156 disjoint, there are at most four chains in this situation. For each chain C_i containing a vertex
 157 v_j , we add the geodesic path connecting the endpoints of C_i to Γ . Therefore, Γ consists
 158 of $O(1)$ geodesic paths and each hourglass H_{C_i} has its top and bottom chain separated by
 159 some path of Γ . Since only $O(1)$ additional paths are computed, this can be done in linear
 160 time. ◀

161 A *chord* of P is an edge joining two non-adjacent vertices a and b of P such that $ab \subseteq P$.
 162 Therefore, a chord splits P into two sub-polygons.

163 ► **Lemma 4.** [Rephrase of Lemma 3.4.3 of [2]] Let C_1, \dots, C_r be a set of edge disjoint
 164 transition chains of ∂P that appear in this order when traversing clockwise the boundary of
 165 P . Then each chord of P appears in $O(1)$ hourglasses among H_{C_1}, \dots, H_{C_r} .

166 **Proof.** Note that chords can only appear on walls of hourglasses. Because hourglasses are
 167 open, any chord must be an edge on exactly one wall of each of these hourglasses. Assume,
 168 for the sake of contradiction, that there exists two points $s, t \in P$ whose chord st is in three
 169 hourglasses H_{C_i}, H_{C_j} and H_{C_k} (for some $1 \leq i < j < k \leq r$) such that s visited before t
 170 when going from the top chain to the bottom one along the walls of the three hourglasses.
 171 Let s_i and t_i be the points in the in the top and bottom chains of H_{C_i} , respectively, such
 172 that $\pi(s_i, t_i)$ is the wall of H_{C_i} that contains st (analogously, we define s_k and t_k)

173 Because C_j lies in between C_i and C_k , Lemma 2 implies that the bottom chain of C_j
 174 appears between the bottom chains of C_i and C_k . Therefore, C_j lies between s_i and s_k and
 175 the bottom chain of H_{C_j} lies between t_i and t_k . That is, for each $x \in C_j$ and each y in the
 176 bottom chain of H_{C_j} , the geodesic path $\pi(x, y)$ is “sandwiched” by the paths $\pi(s_i, t_i)$ and
 177 $\pi(s_k, t_k)$. In particular, $\pi(x, y)$ contains st for each pair of points in the top and bottom
 178 chain of H_{C_j} . However, this implies that the hourglass H_{C_j} is not open—a contradiction
 179 that comes from assuming that st lies in the wall of three open hourglasses, when this wall
 180 is traversed from the top chain to the bottom chain. Analogous arguments can be used to
 181 bound the total number of walls that contain the edge st (when traversed in any direction)
 182 to $O(1)$. ◀

183 ► **Lemma 5.** Let x, u, y, v be four vertices of P that appear in this cyclic order in a clockwise
 184 traversal of ∂P . Given the shortest-path trees T_x and T_y of x and y in P , respectively, such
 185 that T_x and T_y can answer lowest common ancestor (LCA) queries in $O(1)$ time, we can
 186 compute the path $\pi(u, v)$ in $O(|\pi(u, v)|)$ time. Moreover, all edges of $\pi(u, v)$, except perhaps
 187 one, belong to $T_x \cup T_y$.

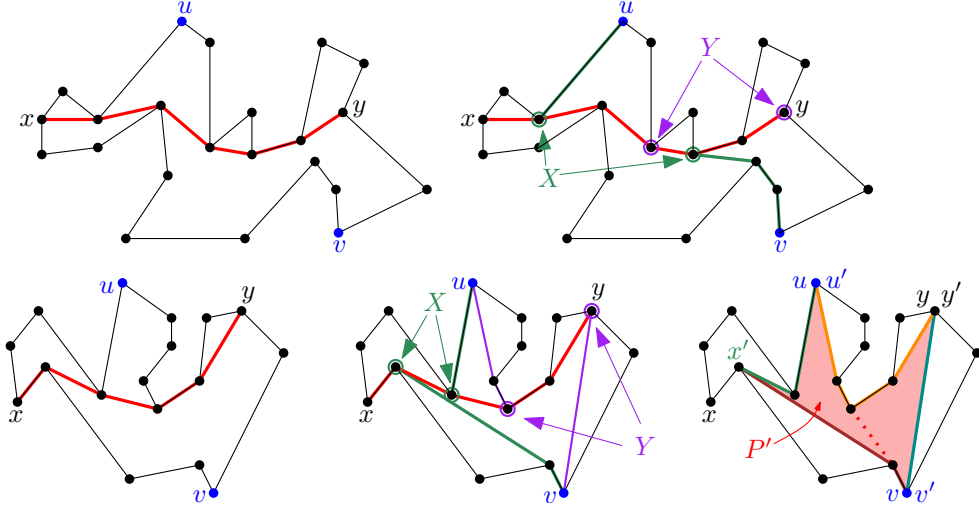
188 **Proof.** Let X (resp. Y) be the set containing the LCA in T_x (resp. T_y) of u, y , and of v, y
 189 (resp. u, x and x, y). Note that the points of $X \cup Y$ lie on the path $\pi(x, y)$ and can be
 190 computed in $O(1)$ time by hypothesis. Moreover, using LCA queries, we can decide their
 191 order along the path $\pi(x, y)$ when traversing it from x to y . (Both X and Y could consist of
 192 a single vertex in some degenerate situations). Two cases arise:

193 **Case 1.** If there is a vertex $x^* \in X$ lying after a vertex $y^* \in Y$ along $\pi(x, y)$, then the
 194 path $\pi(u, v)$ contains the path $\pi(y^*, x^*)$. In this case, the path $\pi(u, v)$ is the concatenation of
 195 the paths $\pi(u, y^*)$, $\pi(y^*, x^*)$, and $\pi(x^*, v)$ and that the three paths are contained in $T_x \cup T_y$.
 196 Moreover, $\pi(u, v)$ can be computed in time proportional to its length by traversing along the
 197 corresponding tree; see Figure 2 (top).

198 **Case 2.** In this case the vertices of X appear before the vertices of Y along $\pi(x, y)$. Let
 199 x' (resp. y') be the vertex of X (resp. Y) closest to x (resp. y).

200 Let u' be the last vertex of $\pi(u, x)$ that is also in $\pi(u, y)$. Note that u' can be constructed
 201 by walking from u' towards x until the path towards y diverges. Thus, u' can be computed
 202 in $O(|\pi(u, u')|)$ time. Define v' analogously and compute it in $O(|\pi(v, v')|)$ time.

203 Let P' be the polygon bounded by the geodesic paths $\pi(x', u')$, $\pi(u', y')$, $\pi(y', v')$ and
 204 $\pi(v', x')$. Because the vertices of X appear before those of Y along $\pi(x, y)$, P' is a simple
 205 polygon; see Figure 2 (bottom).



■ **Figure 2** (top) Case 1 of the proof of Lemma 5 where the path $\pi(u, v)$ contains a portion of the path $\pi(x, y)$. (bottom) Case 2 of the proof of Lemma 5 where the path $\pi(u, v)$ has exactly one edge being the tangent of the paths $\pi(u', y')$ and $\pi(v', x')$.

206 In this case the path $\pi(u, y)$ is the union of $\pi(u, u')$, $\pi(u', v')$ and $\pi(v', v)$. Because $\pi(u, u')$
 207 and $\pi(v', v)$ can be computed in time proportional to their length, it suffices to compute
 208 $\pi(u', v')$ in $O(|\pi(u', v')|)$ time.

209 Note that P' is a simple polygon with only four convex vertices x', u', y' and v' , which
 210 are connected by chains of reflex vertices. Thus, the shortest path from x' to y' can have at
 211 most one diagonal edge connecting distinct reflex chains of P' . Since the rest of the points
 212 in $\pi(u', v')$ lie on the boundary of P' and from the fact that each edge of P' is an edge of
 213 $T_x \cup T_y$, we conclude all edges of $\pi(u, v)$, except perhaps one, belong to $T_x \cup T_y$.

214 We want to find the common tangent between the reflex paths $\pi(u', x')$ and $\pi(v', y')$, or
 215 the common tangent of $\pi(u', y')$ and $\pi(v', x')$ as one of them belongs to the shortest path
 216 $\pi(u', v')$. Assume that the desired tangent lies between the paths $\pi(u', x')$ and $\pi(v', y')$.
 217 Since these paths consist only of reflex vertices, the problem can be reduced to finding the
 218 common tangent of two convex polygons. By slightly modifying the linear time algorithm to
 219 compute this tangents, we can make it run in $O(|\pi(u', v')|)$ time.

220 Since we do not know if the tangent lies between the paths $\pi(u', x')$ and $\pi(v', y')$, we
 221 process the chains $\pi(u', y')$ and $\pi(v', x')$ in parallel and stop when finding the desired tangent.
 222 Consequently, we can compute the path $\pi(u, v)$ in time proportional to its length. ◀

► **Lemma 6.** Let P be a simple polygon with n vertices. Given k disjoint transition chains C_1, \dots, C_k of ∂P , it holds that

$$\sum_{i=1}^k |H_{C_i}| = O(n).$$

223 **Proof.** Because the given transition chains are disjoint, Lemma 2 implies that the bottom
 224 chains of their respective hourglasses are also disjoint. Therefore, the sum of the complexities
 225 of all the top and bottom chains of these hourglasses is $O(n)$. To bound the complexity of
 226 their walls we use Lemma 4. Since no chord is used more than a constant number of times,
 227 it suffices to show that the total number of chords used by all these hourglasses is $O(n)$.

To prove this, we use Lemma 3 to construct $O(1)$ *split chains* $\gamma_1, \dots, \gamma_t$ such that for each $1 \leq i \leq k$, there is a split chain γ_j that separates the top and bottom chains of H_{C_i} . For each $1 \leq j \leq t$, let

$$\mathcal{H}^j = \{H_{C_i} : \text{the top and bottom chain of } H_{C_i} \text{ are separated by } \gamma_j\}.$$

Since the complexity of the shortest-path trees of the endpoints of γ_j is $O(n)$ [10], and from the fact that the chains C_1, \dots, C_k are disjoint, Lemma 5 implies that the total number of edges in all the hourglasses of \mathcal{H}^j is $O(n)$. Moreover, because each of these edges appears in $O(1)$ hourglasses among C_1, \dots, C_k , we conclude that

$$\sum_{H \in \mathcal{H}^j} |H| = O(n).$$

228 Since we have only $O(1)$ split chains, our result follows. ◀

229 2.2 Funnels

230 Let $C = (p_0, \dots, p_k)$ be a chain of ∂P and let v be a vertex of P not in C . The *funnel* of v to
 231 C , denoted by $S_v(C)$, is the simple polygon bounded by C , $\pi(p_k, v)$ and $\pi(v, p_0)$; see Figure 3
 232 (a). Note that the paths $\pi(v, p_k)$ and $\pi(v, p_0)$ may coincide for a while before splitting into
 233 disjoint chains. See Lee and Preparata [15] or Guibas et al. [10] for more details on funnels.

234 A subset $R \subset P$ is *geodesically convex* if for every $x, y \in R$, the path $\pi(x, y)$ is contained
 235 in R . This funnel $S_v(C)$ is also known as the geodesic convex hull of C and v , i.e., the
 236 minimum geodesically convex set that contains v and C .

237 Given two points $x, y \in P$, the (geodesic) *bisector* of x and y is the set of points contained
 238 in P that are equidistant from x and y . This bisector is a curve, contained in P , that
 239 consists of circular arcs and hyperbolic arcs. Moreover, this curve intersects ∂P only at its
 240 endpoints [1, Lemma 3.22].

241 The (farthest) *Voronoi region* of a vertex v of P is the set of points $R(v) = \{x \in P : F_P(x) = |\pi(x, v)|\}$ (including boundary points).

243 ► **Lemma 7.** *Let v be a vertex of P and let C be a transition chain such $R(v) \cap \partial P \subseteq C$
 244 and $v \notin C$. Then, $R(v)$ is contained in the funnel $S_v(C)$*

245 **Proof.** Let a and b be the endpoints of C such that $a, b, f(a)$ and $f(b)$ appear in this order
 246 in a clockwise traversal of ∂P . Because $R(v) \cap \partial P \subseteq C$, we know that v lies between $f(a)$
 247 and $f(b)$.

248 Let α (resp. β) be the bisector of v and $f(a)$ (resp. $f(b)$). Let h_a (resp. h_b) be the set of
 249 points of P that are farther from v than from $f(a)$ (resp. $f(b)$). Note that α is the boundary
 250 of h_a while β bounds h_b .

251 By definition, we know that $R(v) \subseteq h_a \cap h_b$. Therefore, it suffices to show that $h_a \cap h_b \subseteq S_v(C)$.
 252 Assume for a contradiction that there is a point of $h_a \cap h_b$ lying outside of $S_v(C)$.
 253 By continuity of the geodesic distance, the boundaries of $h_a \cap h_b$ and $S_v(C)$ must intersect.
 254 Because $a \notin h_a$ and $b \notin h_b$, both bisectors α and β must have an endpoint on the edge
 255 ab . Since the boundaries of $h_a \cap h_b$ and $S_v(C)$ intersect, we infer that $\beta \cap \pi(v, b) \neq \emptyset$ or
 256 $\alpha \cap \pi(v, a) \neq \emptyset$. Without loss of generality, assume that there is a point $w \in \beta \cap \pi(v, b)$, the
 257 case where w lies in $\alpha \cap \pi(v, a)$ is analogous.

Since $w \in \beta$, we know that $|\pi(w, v)| = |\pi(w, f(b))|$. By the triangle inequality and since w cannot be a vertex of P as w intersects ∂P only at its endpoints, we get that

$$|\pi(b, f(b))| < |\pi(b, w)| + |\pi(w, f(b))| = |\pi(b, w)| + |\pi(w, v)| = |\pi(b, v)|.$$

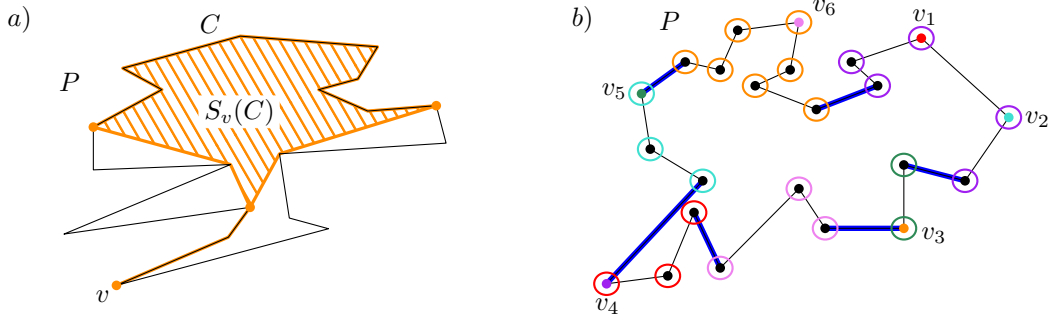


Figure 3 a) The funnel $S_v(C)$ of a vertex v and a chain C contained in ∂P are depicted. b) Each vertex of the boundary of P is assigned with a farthest neighbor which is then marked. The boundary is then decomposed into vertex disjoint chains, each associated with a marked vertex, joined by transition edges (blue) whose endpoints have different farthest neighbors.

Which implies that b is farther from v than from $f(b)$ —a contradiction that comes from assuming that $h_a \cap h_b$ is not contained in $S_v(C)$. \blacktriangleleft

3 Decomposing the boundary

In this section, we decompose the boundary of P into consecutive vertices that share the same farthest neighbor and edges of P whose endpoints have distinct farthest neighbors.

Using a result from Hershberger and Suri [13], in $O(n)$ time we can compute the farthest neighbor of each vertex of P . Recall that the farthest neighbor of each vertex of P is always a convex vertex of P [3] and is unique by our general position assumption.

We mark the vertices of P that are farthest neighbors of at least one vertex of P . Let M denote the set of marked vertices of P (clearly this set can be computed in $O(n)$ time after applying the result of Hershberger and Suri). In other words, M contains all vertices of P whose Voronoi region contains at least one vertex of P .

Given a vertex v of P , the vertices of P whose farthest neighbor is v appear contiguously along ∂P [2]. Therefore, after computing all these farthest neighbors, we effectively split the boundary into subchains, each associated with a different vertex of M ; see Figure 3 (b).

Let a and b be the endpoints of a transition edge of ∂P such that a appears before b in the clockwise order along ∂P . Because ab is a transition edge, we know that $f(a) \neq f(b)$. Recall that we have computed $f(a)$ and $f(b)$ in the previous step and note that $f(a)$ appears also before $f(b)$ along this clockwise order. For every vertex v that lies between $f(a)$ and $f(b)$ in the bottom chain of H_{ab} , we know that there cannot be a vertex u of P such that $f(u) = v$. As proved by Aronov et al. [2, Corollary 2.7.4], if there is a point x on ∂P whose farthest neighbor is v , then x must lie on the open segment (a, b) . In other words, the Voronoi region $R(v)$ restricted to ∂P is contained in (a, b) .

4 Building hourglasses

Let E be the set of transition edges of ∂P . Given a transition edge $ab \in E$, we say that H_{ab} is a *transition hourglass*. In order to construct the triangle cover of P , we construct the transition hourglass of each transition edge of E . By Lemma 6, we know that $\sum_{ab \in E} |H_{ab}| = O(n)$. Therefore, our aim is to compute the cover in time proportional to the size of H_{ab} .

By Lemma 3 we can compute a set of $O(1)$ separating paths such that for each transition

edge ab , the transition hourglass H_{ab} is separated by one (or more) paths in this set. For each endpoint of the $O(1)$ separating paths we compute its shortest-path tree [10]. In addition, we preprocess these trees in linear time to support LCA queries [12]. Both computations need linear time per endpoint and use $O(n)$ space. Since we do this process for a constant number of endpoints, overall this preprocessing takes $O(n)$ time.

Let γ be a separating path whose endpoints are x and y . Note that γ separates the boundary of P into two chains S and S' such that $S \cup S' = \partial P$. Let $\mathcal{H}(\gamma)$ be the set of each transition hourglass separated by γ whose transition edge is contained in S (whenever an hourglass is separated by more than one path, we pick one arbitrarily). Note that we can classify all transition hourglasses into the sets $\mathcal{H}(\gamma)$ in $O(n)$ time (since $O(1)$ separating paths are considered).

We claim that we can compute all transition hourglass of $\mathcal{H}(\gamma)$ in $O(n)$ time. By construction, the wall of each of these hourglasses consists of a (geodesic) path that connects a point in S with a point in S' . Let $u \in S$ and $v \in S'$ be two vertices such that $\pi(u, v)$ is the wall of a hourglass in $\mathcal{H}(\gamma)$. Because LCA queries can be answered in $O(1)$ time [12], Lemma 5 allows us to compute this path in $O(|\pi(u, v)|)$ time. Therefore, we can compute all hourglasses of $\mathcal{H}(\gamma)$ in $O(\sum_{H \in \mathcal{H}(\gamma)} |H| + n) = O(n)$ time by Lemma 6. Because only $O(1)$ separating paths are considered, we obtain the following result.

► **Lemma 8.** *We can construct the transition hourglass of all transition edges of P in $O(n)$ time.*

5 Covering the polygon with apexed triangles

An *apexed triangle* $\Delta = (a, b, c)$ with *apex* a is a triangle contained in P with an associated distance function $g_\Delta(x)$, called the *apex function* of Δ , such that (1) a is a vertex of P , (2) $b, c \in \partial P$, and (3) there is a vertex w of P , called the *definer* of Δ , such that

$$g_\Delta(x) = \begin{cases} -\infty & \text{if } x \notin \Delta \\ |xa| + |\pi(a, w)| = |\pi(x, w)| & \text{if } x \in \Delta \end{cases}$$

In this section, we show how to find a set of $O(n)$ apexed triangles of P such that the upper envelope of their apex functions coincides with $F_P(x)$. To this end, we first decompose the transition hourglasses into apexed triangles that encode all the geodesic distance information inside them. For each marked vertex $v \in M$ we construct a funnel that contains the Voronoi region of v . We then decompose this funnel into apexed triangles that encode the distance from v .

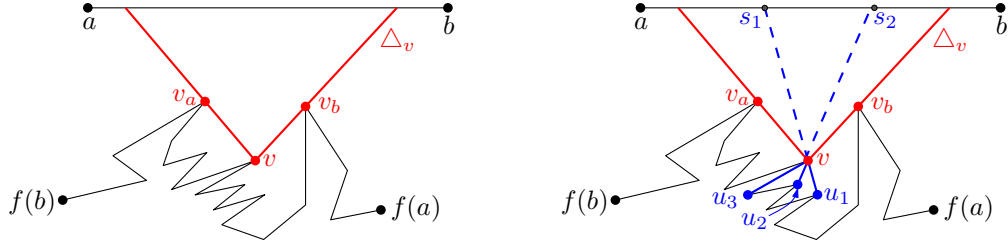
5.1 Inside the transition hourglass

Let ab be a transition edge of P such that b is the clockwise neighbor of a along ∂P . Let B_{ab} denote the bottom chain of H_{ab} after removing its endpoints. As noticed above, a point on ∂P can be farthest from a vertex in B_{ab} only if it lies in the open segment ab . That is, if v is a vertex of B_{ab} such that $R(v) \neq \emptyset$, then $R(v) \cap \partial P \subset ab$.

In fact, not only this Voronoi region is inside H_{ab} when restricted to the boundary of P , but also $R(v) \subset H_{ab}$. The next result follows trivially from Lemma 7.

► **Corollary 9.** *Let v be a vertex of B_{ab} . If $R(v) \neq \emptyset$, then $R(v) \subset H_{ab}$.*

Our objective is to compute $O(|H_{ab}|)$ apexed triangles that cover H_{ab} , each with its distance function, such that the upper envelope of these apex functions coincides with $F_P(x)$ restricted to H_{ab} where it “matters”.



■ **Figure 4** (left) A vertex v visible from the segment ab lying on the bottom chain of H_{ab} , and the triangle Δ_v which contains the portion of ab visible from v . (right) The children u_1 and u_2 of v are visible from ab while u_3 is not. The triangle Δ_v is split into apexed triangles by the rays going from u_1 and u_2 to v .

325 The same approach was already used by Pollack et al. in [22, Section 3]. Given a segment
 326 contained in the interior of P , they show how to compute a linear number of apexed triangles
 327 such that $F_P(x)$ coincides with the upper envelope of the corresponding apex functions in
 328 the given segment.

329 While the construction we follow is analogous, we use it in the transition hourglass H_{ab}
 330 instead of the full polygon P . Therefore, we have to specify what is the relation between the
 331 upper envelope of the computed functions and $F_P(x)$. We will show that the upper envelope
 332 of the apex functions computed in H_{ab} coincides with $F_P(x)$ inside the Voronoi region $R(v)$
 333 of every vertex $v \in B_{ab}$.

334 Let T_a and T_b be the shortest-path trees in H_{ab} from a and b , respectively. Assume
 335 that T_a and T_b are rooted at a and b , respectively. We can compute these trees in $O(|H_{ab}|)$
 336 time [10]. For each vertex v between $f(a)$ and $f(b)$, let v_a and v_b be the neighbors of v
 337 in the paths $\pi(v, a)$ and $\pi(v, b)$, respectively. We say that a vertex v is *visible* from ab if
 338 $v_a \neq v_b$. Note that if a vertex is visible, then the extension of these segments must intersect
 339 the top segment ab . Therefore, for each visible vertex v , we obtain a triangle Δ_v as shown in
 340 Figure 4.

341 We further split Δ_v into a series of triangles with apex at v as follows: Let u be a child
 342 of v in either T_a or T_b . As noted by Pollack et al., v can be of three types, either (1) u is not
 343 visible from ab (and is hence a child of v in both T_a and T_b); or (2) u is visible from ab , is a
 344 child of v only in T_b , and v_bvu is a left turn; or (3) u is visible from ab , is a child of v only in
 345 T_a , and v_avu is a right turn.

346 Let u_1, \dots, u_{k-1} be the children of v of type (2) sorted in clockwise order around v . Let
 347 $c(v)$ be the maximum distance from v to any invisible vertex in the subtrees of T_a and T_b
 348 rooted at v ; if no such vertex exists, then $c(v) = 0$. Define a function $d_l(v)$ on each vertex v
 349 of H_{ab} in a recursive fashion as follows: If v is invisible from ab , then $d_l(v) = c(v)$. Otherwise,
 350 let $d_l(v)$ be the maximum of $c(v)$ and $\max\{d_l(u_i) + |u_iv| : u_i \text{ is a child of } v \text{ of type (2)}\}$.
 351 Similarly we define a symmetric function $d_r(v)$ using the children of type (3) of v .

For each $1 \leq i \leq k-1$, extend the segment u_iv past v until it intersects ab at a point
 s_i . Let s_0 and s_k be the intersections of the extensions of vv_a and vv_b with the segment ab .
 We define then k triangles contained in Δ_v as follows. For each $0 \leq i \leq k-1$, consider the
 triangle $\Delta(s_i, v, s_{i+1})$ whose associated apexed (left) function is

$$f_i(x) = |xv| + \max_{j > i} \{c(v), |vu_j| + d_l(u_j)\}.$$

352 In a symmetric manner, we define a set of apexed triangles induced by the type (3) children
 353 of v and their respective apexed (right) functions.

Let g_1, \dots, g_r and $\Delta_1, \dots, \Delta_r$ respectively be an enumeration of all the generated apex functions and triangles such that g_i is defined in the triangle Δ_i . Because each function is determined uniquely by a pair of adjacent vertices in T_a or in T_b , and since these trees have $O(|H_{ab}|)$ vertices, we conclude that $r = O(|H_{ab}|)$.

Note that for each $1 \leq i \leq r$, the triangle Δ_i has two vertices on the segment ab and a third vertex, say a_i , called its *apex* such that for each $x \in \Delta_i$, $g_i(x) = |\pi(x, w_i)|$ for some vertex w_i of H_{ab} . We refer to w_i as the *definer* of Δ_i . Intuitively, Δ_i defines a portion of the geodesic distance function from w_i in a constant complexity region.

► **Lemma 10.** *Given a transition edge ab of P , we can compute a set \mathcal{A}_{ab} of $O(|H_{ab}|)$ apexed triangles in $O(|H_{ab}|)$ time with the property that for any point $p \in P$ such that $f(p) \in B_{ab}$, there is an apexed triangle $\Delta \in \mathcal{A}_{ab}$ with apex function g and definer equal to $f(p)$ such that*

1. $p \in \Delta$ and
2. $g(p) = F_P(p)$.

Proof. Because $p \in R(f(p))$, Lemma 9 implies that $p \in H_{ab}$. Consider the path $\pi(p, f(p))$ and let v be the neighbor of p along this path. By construction of \mathcal{A}_{ab} , there is a triangle $\Delta \in \mathcal{A}_{ab}$ apexed at v with definer w that contains p . The apex function $g(x)$ of Δ encodes the geodesic distance from x to w . Because $F_P(x)$ is the upper envelope of all the geodesic functions, we know that $g(p) \leq F_P(p)$.

To prove the other inequality, note that if $v = f(p)$, then trivially $g(p) = |pv| + |\pi(v, w)| \geq |pv| = |\pi(p, f(p))| = F_P(p)$. Otherwise, let z be the next vertex after v in the path $\pi(p, f(p))$. Three cases arise:

(a) If z is invisible from ab , then so is $f(p)$ and hence,

$$|\pi(p, f(p))| = |pv| + |\pi(v, f(p))| \leq |pv| + c(v) \leq g(p).$$

(b) If z is a child of type (2), then z plays the role of some child u_j of v in the notation used during the construction. In this case:

$$|\pi(p, f(p))| = |pv| + |vz| + |\pi(z, f(p))| \leq |pv| + |vu_j| + d_l(u_j) \leq g(p).$$

(c) If z is a child of type (3), then analogous arguments hold using the (right) distance d_r .

Therefore, regardless of the case $F_P(p) = |\pi(p, f(p))| \leq g(p)$.

To bound the running time, note that the recursive functions d_l, d_r and c can be computed in $O(|T_a| + |T_b|)$ time. Then, for each vertex visible from ab , we can process it in time proportional to its degree in T_a and T_b . Because the sum of the degrees of all vertices in T_a and T_b is $O(|T_a| + |T_b|)$ and from the fact that both $|T_a|$ and $|T_b|$ are $O(|H_{ab}|)$, we conclude that the total running time to construct \mathcal{A}_{ab} is $O(|H_{ab}|)$. ◀

In other words, Lemma 10 says that no information on farthest neighbors is lost if we only consider the functions in \mathcal{A}_{ab} within H_{ab} . In the next section we use a similar approach to construct a set of apexed triangles (and their corresponding apex functions), so as to encode the distance from the vertices of M .

5.2 Inside the funnels of marked vertices

Recall that for each marked vertex $v \in M$, we know at least of one vertex on ∂P such that v is its farthest neighbor. For any marked vertex v , let u_1, \dots, u_{k-1} be the vertices of P such that $v = f(u_i)$ and assume that they appear in this order when traversing ∂P clockwise. Let u_0 and u_k be the neighbors of u_1 and u_{k-1} other than u_2 and u_{k-2} , respectively. Note that

both u_0u_1 and $u_{k-1}u_k$ are transition edges of P . Thus, we can assume that their transition hourglasses have been computed.

Let $C_v = (u_0, \dots, u_k)$ and consider the funnel $S_v(C_v)$. We call C_v the *main chain* of $S_v(C_v)$ while $\pi(u_k, v)$ and $\pi(v, u_0)$ are referred to as the *walls* of the funnel. Because $v = f(u_1) = f(u_{k-1})$, we know that v is a vertex of both $H_{u_0u_1}$ and $H_{u_{k-1}u_k}$. By definition, we have $\pi(v, u_0) \subset H_{u_0u_1}$ and $\pi(v, u_k) \subset H_{u_{k-1}u_k}$. Thus, we can explicitly compute both paths $\pi(v, u_0)$ and $\pi(v, u_k)$ in $O(|H_{u_0u_1}| + |H_{u_{k-1}u_k}|)$ time. So, overall, the funnel $S_v(C_v)$ can be constructed in $O(k + |H_{u_0u_1}| + |H_{u_{k-1}u_k}|)$ time. Recall that, by Lemma 6, the total sum of the complexities of the transition hourglasses is $O(n)$. In particular, we can bound the total time needed to construct the funnels of all marked vertices by $O(n)$.

Since the complexity of the walls of these funnels is bounded by the complexity of the transition hourglasses used to compute them, we get that

$$\sum_{v \in M} |S_v(C_v)| = O\left(n + \sum_{ab \in E} |H_{ab}|\right) = O(n).$$

► **Lemma 11.** *Let x be a point in P . If $v = f(x)$ is a vertex of M , then $x \in S_v(C_v)$.*

Proof. Since $f(u_0) \neq f(u_k)$, C_v is a transition chain. Moreover, C_v contains $R(v) \cap \partial P$ by definition. Therefore, Lemma 7 implies that $R(v) \subset S_v(C_v)$. Since $v = f(x)$, we know that $x \in R(v)$ and hence that $x \in S_v(C_v)$. ◀

We now proceed to split a given funnel into $O(|S_v(C_v)|)$ apexed triangles that encode the distance function from v . To this end, we compute the shortest-path tree T_v of v in $S_v(C_v)$ in $O(|S_v(C_v)|)$ time [11]. We consider the tree T_v to be rooted at v and assume that for each node u of this tree we have stored the geodesic distance $|\pi(u, v)|$.

Start an Eulerian tour from v walking in a clockwise order of the edges. Let w_1 be the first leaf of T_v found, and let w_2 and w_3 be the next two vertices visited in the traversal. Two cases arise:

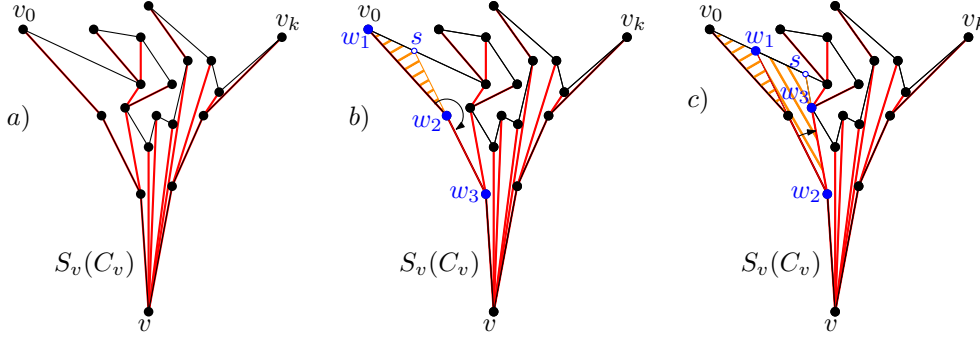
Case 1: w_1, w_2, w_3 makes a right turn. We define s as the first point hit by the ray apexed at w_2 that shoots in the direction opposite to w_3 .

We claim that w_1 and s lie on the same edge of the boundary of $S_v(C_v)$. Otherwise, there would be a vertex u visible from w_2 inside the wedge with apex w_2 spanned by w_1 and w_3 . Note that the first edge of the path $\pi(u, v)$ is the edge uw_2 . Therefore, uw_2 belongs to the shortest-path T_v contradicting the Eulerian order in which the vertices of this tree are visited as u should be visited before w_3 . Thus, s and w_1 lie on the same edge and s can be computed in $O(1)$ time.

At this point, we construct the apexed triangle $\Delta(w_2, w_1, s)$ apexed at w_2 with apex function $g(x) = |xw_2| + |\pi(w_2, v)|$. We modify tree T_v by removing the edge w_1w_2 and replacing the edge w_3w_2 by the edge w_3s ; see Figure 5.

Case 2: w_1, w_2, w_3 makes a left turn and w_1 and w_3 are adjacent, then if w_1 and w_3 lie on the same edge of ∂P , we construct an apexed triangle $\Delta(w_2, w_1, w_3)$ apexed at w_2 with apex function $g(x) = |xw_2| + |\pi(w_2, v)|$. Otherwise, let s be the first point of the boundary of $S_v(C_v)$ hit by the ray shooting from w_3 in the direction opposite to w_2 .

By the same argument as above, we can show that w_1 and s lie on the same edge of the boundary of $S_v(C_v)$ (and thus, we can compute s in $O(1)$ time). We construct an apexed triangle $\Delta(w_2, w_1, s)$ apexed at w_2 with apex function $g(x) = |xw_2| + |\pi(w_2, v)|$. We modify the tree T_v by removing the edge w_1w_2 and adding the edge w_3s ; see Figure 5 for an illustration.



■ **Figure 5** The funnel $S_v(C_v)$ and the shortest-path tree from v are depicted in (a). The two cases of the algorithm described in Lemma 12 are shown in (b) and (c).

432 ► **Lemma 12.** *The above procedure runs in $O(|S_v(C_v)|)$ time and computes $O(|S_v(C_v)|)$*
 433 *interior disjoint apexed triangles such that their union covers $S_v(C_v)$. Moreover, for each*
 434 *point $x \in R(v)$, there is an apexed triangle Δ with apex function $g(x)$ such that (1) $x \in \Delta$*
 435 *and (2) $g(x) = F_P(x)$.*

436 **Proof.** The above procedure splits $S_v(C_v)$ into apexed triangles, such that their apex function
 437 in each of them is defined as the geodesic distance to v . By Lemma 11, if $x \in R(v)$, then
 438 $x \in S_v(C_v)$. Therefore, there is an apexed triangle Δ with apex function $g(x)$ such that
 439 $x \in \Delta$ and $g(x) = |\pi(x, v)| = F_P(x)$. Consequently, we obtain properties (1) and (2).

440 We now bound the running time of the algorithm. The shortest-path tree T_v from v
 441 is computed in $O(|S_v(C_v)|)$ time [10]. For each leaf of T_v we need a constant number of
 442 operations to determine in which of the cases we are in (and to treat it as well). Therefore, it
 443 suffices to bound the number of times these steps are performed. Note that a leaf is removed
 444 from the tree in each iteration. Since the number of leaves strictly decreases each time we
 445 are in Case 2, this step cannot happen more than $O(|S_v(C_v)|)$ times. In Case 1 a new leaf
 446 is added if w_1 and w_3 do not lie on the same edge of ∂P . However, the number of leaves
 447 that can be added throughout is at most the number of edges of T_v . Note that the edges
 448 added by either Case 1 or 2 are chords of the polygon and hence do not generate further
 449 leaves. Because $|T_v| = O(|S_v(C_v)|)$, we conclude that both Case 1 and 2 are only executed
 450 $O(|S_v(C_v)|)$ times. ◀

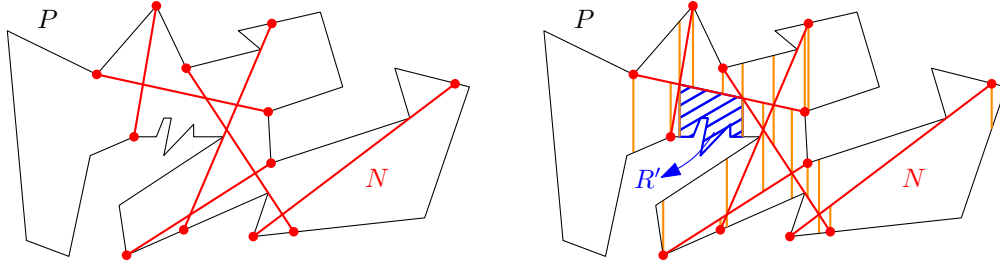
451 6 Prune and search

452 With the tools introduced in the previous sections, we can proceed to give the prune and
 453 search algorithm to compute the geodesic center. The idea of the algorithm is to partition P
 454 into $O(1)$ cells, determine on which cell of P the center lies and recurse on that cell as a new
 455 subproblem with smaller complexity.

456 Naturally, we can discard all apexed triangles that do not intersect the new cell containing
 457 the center. Using the properties of the cutting, we can show that both the complexity of the
 458 cell containing the center, and the number of apexed triangles that intersect it decrease by
 459 a constant fraction in each iteration of the algorithm. This process is then repeated until
 460 either of the two objects has constant descriptive size.

461 Let τ be the set all apexed triangles computed in previous sections. Lemmas 6 and 12
 462 directly provide a bound on the complexity of τ .

463 ► **Corollary 13.** *The set τ consists of $O(n)$ apexed triangles.*



■ **Figure 6** The ϵ -net N splits P into $O(1)$ sub-polygons that are further refined into a 4-cell decomposition using $O(1)$ ray-shooting queries from the vertices of the arrangement defined by N .

Let $\phi(x)$ be the upper envelope of the apex functions of every triangle in τ (i.e., $\phi(x) = \max\{g_i(x) : g_i(x) \in \tau, x \in \Delta_i\}$). The following result is a direct consequence of Lemmas 10 and 12, and shows that the $O(n)$ apexed triangles of τ not only cover P , but their apex functions suffice to reconstruct the function $F_P(x)$.

► **Lemma 14.** *The functions $\phi(x)$ and $F_P(x)$ coincide in the domain of points of P , i.e., for each $p \in P$, $\phi(p) = F_P(p)$.*

Given a chord C of P a *half-polygon* of P is one of the two simple polygons in which C splits P . A *4-cell* of P is a simple polygon obtained as the intersection of at most four half-polygons. Because a 4-cell is the intersection of geodesically convex sets, it is also geodesically convex.

Let R be a 4-cell of P and let τ_R be the set of apexed triangles of τ that intersect R . Let $m_R = \max\{|R|, |\tau_R|\}$. Recall that, by construction of the apexed triangles, for each triangle of τ_R at least one and at most two of its boundary segments is a chord of P . Let \mathcal{C} be the set containing all chords that belong to the boundary of a triangle of τ_R . Therefore, $|\tau_R| \leq |\mathcal{C}| \leq 2|\tau_R|$.

To construct an ϵ -net of \mathcal{C} , we need some definitions (for more information on ϵ -nets refer to [17]). Let φ be the set of all open 4-cells of P . For each $t \in \varphi$, let $\mathcal{C}_t = \{C \in \mathcal{C} : C \cap t \neq \emptyset\}$ be the set of chords of \mathcal{C} induced by t . Finally, let $\varphi_{\mathcal{C}} = \{\mathcal{C}_t : t \in \varphi\}$ be the family of subsets of \mathcal{C} induced by φ .

Let $\epsilon > 0$ (the exact value of ϵ will be specified later). Consider the range space $(\mathcal{C}, \varphi_{\mathcal{C}})$ defined by \mathcal{C} and $\varphi_{\mathcal{C}}$. Because the VC-dimension of this range space is finite, we can compute an ϵ -net N of $(\mathcal{C}, \varphi_{\mathcal{C}})$ in $O(n/\epsilon) = O(n)$ time [17]. The size of N is $O(\frac{1}{\epsilon} \log \frac{1}{\epsilon}) = O(1)$ and its main property is that any 4-cell that does not intersect a chord of N will intersect at most $\epsilon|\mathcal{C}|$ chords of \mathcal{C} .

Observe that N partitions R into $O(1)$ sub-polygons (not necessarily 4-cells). We further refine this partition by performing a 4-cell decomposition. That is, we shoot vertical rays up and down from each endpoint of N , and from the intersection point of any two segments of N , see Figure 6. Overall, this partitions R into $O(1)$ 4-cells such that each either (i) is a convex polygon contained in P of at most four vertices, or otherwise (ii) contains some chain of ∂P . Since $|N| = O(1)$, the whole decomposition can be computed in $O(m_R)$ time (the intersections between segments of N are done in constant time, and for the ray shooting operations we walk along the boundary of R once).

In order to determine which 4-cell contains the geodesic center of P , we extend each edge of a 4-cell to a chord C . This can be done with two ray-shooting queries (each of which takes $O(m_R)$ time). We then use the chord-oracle from Pollack et al. [22, Section 3] to decide which side of C contains c_P . The only requirement of this technique is that the function

$F_P(x)$ coincides with the upper envelope of the apex functions when restricted to C . Which is true by Lemma 14 and from the fact that τ_R consists of all the apexed triangles of τ that intersect R .

Because the chord-oracle described by Pollack et al. [22, Section 3] runs in linear time on the number of functions defined on C , we can decide in total $O(m_R)$ time on which side of C the geodesic center of P lies. Since our decomposition into 4-cells has constant complexity, we need to perform $O(1)$ calls to the oracle before determining the 4-cell R' that contains the geodesic center of P .

The chord-oracle computes the minimum of $F_P(x)$ restricted to the chord before determining the side containing the minimum. In particular, if c_P lies on any chord bounding R' , then the chord-oracle will find it. Therefore, we can assume that c_P lies in the interior of R' . Moreover, since N is a ε -net, we know that at most $\varepsilon|C|$ chords of C will intersect R' .

Using a similar argument, we can show that the complexity of R' also decreases: since $|C| \leq 2|\tau_R| \leq 2m_R$, we guarantee that at most $2\varepsilon m_R$ apexed triangles intersect R' . Moreover, each vertex of R' is in at least one apexed triangle of τ_R by Lemma 14, and by construction, each apexed triangle can cover at most three vertices. Thus, by the pigeonhole principle we conclude that R' can have at most $6\varepsilon m_R$ vertices. Thus, if we choose $\varepsilon = 1/12$, we guarantee that both the size of the 4-cell R' and the number of apexed triangles in $\tau_{R'}$ are at most $m_R/2$.

In order to proceed with the algorithm on R' recursively, we need to compute the set $\tau_{R'}$ with the at most $\varepsilon|C|$ apexed triangles of τ_R that intersect R' (i.e., prune the apexed triangles that do not intersect with R'). For each apexed triangle $\Delta \in \tau_R$, we can determine in constant time if it intersects R' (either one of the endpoints is in $R' \cap \partial P$ or the two boundaries have non-empty intersection in the interior of P). Overall, we need $O(m_R)$ time to compute the at most $\varepsilon|C|$ triangles of τ_R that intersect R' .

By recursing on R' , we guarantee that after $O(\log m_R)$ iterations, we reduce the size of either τ_R or R' to constant. In the former case, the minimum of $F_P(x)$ can be found by explicitly constructing function ϕ in $O(1)$ time. In the latter case, we triangulate R' and apply the chord-oracle to determine which triangle will contain c_P . The details needed to find the minimum of $\phi(x)$ inside this triangle are giving the next section.

► **Lemma 15.** *In $O(n)$ time we can find either the geodesic center of P or a triangle containing the geodesic center.*

7 Solving the problem restricted to a triangle

In order to complete the algorithm it remains to show how to find the geodesic center of P for the case in which R' is a triangle. If this triangle is in the interior of P , it may happen that several apexed triangles of τ fully contain R' . Thus, the pruning technique used in the previous section cannot be further applied. We solve this case with a different approach.

Recall that $\phi(x)$ denotes the upper envelope of the apex functions of the triangles in τ , and the geodesic center is the point that minimizes ϕ . The key observation is that, as it happened with chords, the function $\phi(x)$ restricted to R' is convex.

Let $\Delta_1, \Delta_2, \dots, \Delta_m$ be the set of $m = O(n)$ apexed triangles of τ that intersect R' . Let $g_i(x) = |xa_i| + \kappa_i$ be the apex function of Δ_i , where a_i and w_i are the apex and the definer of Δ_i , respectively, and $\kappa_i = |\pi(a_i, w_i)|$ is a constant.

By Lemma 14, $\phi(x) = F_P(x)$. Therefore, the problem of finding the center is equivalent to the following optimization problem in \mathbb{R}^3 :

(P1). Find a point $(x, r) \in \mathbb{R}^3$ minimizing r subject to $x \in R'$ and

$$g_i(x) = |xa_i| + \kappa_i \leq r, \text{ if } x \in \triangle_i \text{ for } 1 \leq i \leq m.$$

Thus, we need only to find the solution to (P1) to find the geodesic center of P . A similar optimization was studied by Megiddo in [18]. The main difference being that we have apex functions, defined only in their corresponding apexed triangles, instead of functions defined in the entire plane.

We use some remarks described by Megiddo in order to simplify the description of (P1). To simplify the formulas, we square the equations:

$$\|x\|^2 - 2x \cdot a_i + \|a_i\|^2 = |xa_i|^2 \leq (r - \kappa_i)^2 = r^2 - 2r\kappa_i + \kappa_i^2.$$

And finally for each $1 \leq i \leq m$, we define the function $h_i(x, r)$ as follows:

$$h_i(x, r) = \|x\|^2 - 2x \cdot a_i + \|a_i\|^2 - r^2 + 2r\kappa_i - \kappa_i^2 \leq 0$$

Therefore, our optimization problem can be reformulated as:

(P2). Find a point $(x, r) \in \mathbb{R}^3$ such that r is minimized subject to $x \in R'$ and

$$h_i(x, r) \leq 0, \text{ if } x \in \triangle_i \text{ for } 1 \leq i \leq m.$$

Although the functions $h_i(x, r)$ are not linear, they all have the same non-linear terms. Therefore, for $i \neq j$, we get that $h_i(x, r) = h_j(x, r)$ defines a *separating plane*

$$\gamma_{i,j} = \{(x, r) \in \mathbb{R}^3 : 2(\kappa_i - \kappa_j)r - 2(a_i - a_j) \cdot x + \|a_i\|^2 - \|a_j\|^2 - \kappa_i^2 + \kappa_j^2 = 0\}$$

As noted by Megiddo, this separating plane has the following property: If the solution (x, r) to our optimization problem is known to lie to one side of $\gamma_{i,j}$, then we know that one of the constraints is redundant.

In Megiddo's problem, it sufficed to have a *side-decision oracle* to determine on which side of a plane $\gamma_{i,j}$ the solution lies. Megiddo showed how to implement this oracle in a way that the running time is proportional to the number of constraints [18].

Once we have such an oracle, we can proceed with the prune and search similar to the one introduced in Section 6: pair the functions arbitrarily, and consider the set of $m/2$ separating planes defined by these pairs. For some constant r , compute a $1/r$ -cutting in \mathbb{R}^3 of the separating planes. A $1/r$ -cutting is a partition of the plane into $O(r^2)$ convex regions each of which is of constant size and intersects at most $m/2r$ separating planes. A cutting of planes can be computed in linear time in \mathbb{R}^3 for any $r = O(1)$ [16]. After computing the cutting, determine in which of the regions the minimum lies by performing $O(1)$ calls to the side-decision oracle. Because at least $(r - 1)m/2r$ separating planes do not intersect this constant size region, for each of them we can discard one of the constraints as it becomes redundant. Repeating this algorithm recursively we obtain a linear running time.

In this paper, we follow a similar approach, but our set of separating planes needs to be extended in order to handle apex functions as they are only defined in a triangular domain. Note that the vertices of each apexed triangle that intersect R' have their endpoints either outside of R' or on its boundary.

7.1 Optimization problem in a convex domain

In this section we describe our algorithm to solve the optimization problem (P2). To this end, we pair the apexed triangles arbitrarily to obtain $m/2$ pairs. By identifying the plane

where P lies with the plane $Z_0 = \{(x, y, z) : z = 0\}$, we can embed each apexed triangle in \mathbb{R}^3 . A *plane-set* is a set consisting of at most five planes in \mathbb{R}^3 . For each pair of apexed triangles (Δ_i, Δ_j) we define a plane-set as follows: For each chord bounding either Δ_i or Δ_j , consider the line extending this chord and the vertical extrusion of this line in \mathbb{R}^3 , i.e., the plane containing this chord orthogonal to Z_0 . Moreover, consider the separating plane $\gamma_{i,j}$. The set containing these planes is the plane-set of the pair (Δ_i, Δ_j) .

Let Γ be the union of all the plane-sets defined by the $m/2$ pairs of apexed triangles. Thus, Γ is a set that consists of $O(m)$ planes. Compute an $1/r$ -cutting of Γ in $O(m)$ time for some constant r to be specified later. Because r is constant, this $1/r$ -cutting splits the space into $O(1)$ convex regions, each bounded by a constant number of planes [16]. By using a side-decision algorithm (to be specified later), we can determine the region Q of the cutting that contains the solution to (P2). Because Q is the region of a $1/r$ -cutting of Γ , we know that at most $|\Gamma|/r$ planes of Γ intersect Q . In particular, at most $|\Gamma|/r$ plane-sets intersect Q and hence, at least $(r - 1)|\Gamma|/r$ plane-sets do not intersect Q .

Let (Δ_i, Δ_j) be a pair such that its plane-set does not intersect Q . Let Q' be the projection of Q on the plane Z_0 . Because the plane-set of this pair does not intersect Q , we know that Q' intersects neither the boundary of Δ_i nor that of Δ_j . Two cases arise:

Case 1. If either Δ_i or Δ_j does not intersect Q' , then we know that their apex function is redundant and we can drop the constraint associated with this apexed triangle.

Case 2. If $Q' \subset \Delta_i \cap \Delta_j$, then we need to decide which constrain to drop. To this end, we consider the separating plane $\gamma_{i,j}$. Notice that inside the vertical extrusion of $\Delta_i \cap \Delta_j$ (and hence in Q), the plane $\gamma_{i,j}$ has the property that if we know its side containing the solution, then one of the constraints can be dropped. Since $\gamma_{i,j}$ does not intersect Q as $\gamma_{i,j}$ belongs to the plane-set of (Δ_i, Δ_j) , we can decide which side of $\gamma_{i,j}$ contains the solution to (P2) and drop one of the constraints.

Regardless of the case if the plane-set of a pair (Δ_i, Δ_j) does not intersect Q , then we can drop one of its constraints. Since at least $(r - 1)|\Gamma|/r$ plane-sets do not intersect Q , we can drop at least $(r - 1)|\Gamma|/r$ constraints. Because $|\Gamma| \geq m/2$ as each plane-set contains at least one plane, by choosing $r = 2$, we are able to drop at least $|\Gamma|/2 \geq m/4$ constraints. Consequently, after $O(m)$ time, we are able to drop $m/4$ apexed triangles. By repeating this process recursively, we end up with a constant size problem in which we can compute the upper envelope of the functions explicitly and find the solution to (P2) using exhaustive search. Thus, the running time of this algorithm is bounded by the recurrence $T(m) = T(3m/4) + O(m)$ which solves to $O(m)$. Because $m = O(n)$, we can find the solution to (P2) in $O(n)$ time.

The last detail is the implementation of the side-decision algorithm. Given a plane γ , we want to decide on which side lies the solution to (P2). To this end, we solve (P2) restricted to γ , i.e., with the additional constraint of $(x, r) \in \gamma$. This approach was used by Megiddo [18], the idea is to recurse by reducing the dimension of the problem. Another approach is to use a slight modification of the chord-oracle described by Pollack et al. [22, Section 3].

Once the solution to (P2) restricted to γ is known, we can follow the same idea used by Megiddo [18] to find the side of γ containing the global solution to (P2). Intuitively, we find the apex functions that define the minimum restricted to γ . Since $\phi(x) = F_P(x)$ is locally defined by this functions, we can decide on which side the minimum lie using convexity. We obtain the following result.

► **Lemma 16.** *Let R' be a convex trapezoid contained in P such that R' contains the geodesic center of P . Given the set of all apexed triangles of τ that intersect R' , we can compute the*

621 geodesic center of P in $O(n)$ time.

622 The following theorem summarizes the result presented in this paper.

623 ► **Theorem 17.** *We can compute the geodesic center of any simple polygon P of n vertices*
 624 *in $O(n)$ time.*

625 — References —

- 626 1 B. Aronov. On the geodesic Voronoi diagram of point sites in a simple polygon. *Algorith-*
 627 *mica*, 4(1-4):109–140, 1989.
- 628 2 B. Aronov, S. Fortune, and G. Wilfong. The furthest-site geodesic Voronoi diagram. *Dis-*
 629 *crete & Computational Geometry*, 9(1):217–255, 1993.
- 630 3 T. Asano and G. Toussaint. Computing the geodesic center of a simple polygon. Technical
 631 Report SOCS-85.32, McGill University, 1985.
- 632 4 S. W. Bae, M. Korman, and Y. Okamoto. The geodesic diameter of polygonal domains.
 633 *Discrete & Computational Geometry*, 50(2):306–329, 2013.
- 634 5 S. W. Bae, M. Korman, and Y. Okamoto. Computing the geodesic centers of a polygonal
 635 domain. In *Proceedings of CCCG*, 2014.
- 636 6 S. W. Bae, M. Korman, Y. Okamoto, and H. Wang. Computing the L_1 geodesic diameter
 637 and center of a simple polygon in linear time. In *Proceedings of LATIN*, pages 120–131,
 638 2014.
- 639 7 B. Chazelle. A theorem on polygon cutting with applications. In *Proceedings of FOCS*,
 640 pages 339–349, 1982.
- 641 8 H. Djidjev, A. Lingas, and J.-R. Sack. An $O(n \log n)$ algorithm for computing the link
 642 center of a simple polygon. *Discrete & Computational Geometry*, 8:131–152, 1992.
- 643 9 H. Edelsbrunner and E. P. Mücke. Simulation of simplicity: a technique to cope with
 644 degenerate cases in geometric algorithms. *ACM Transactions on Graphics*, 9(1):66–104,
 645 1990.
- 646 10 L. Guibas, J. Hershberger, D. Leven, M. Sharir, and R. E. Tarjan. Linear-time algorithms
 647 for visibility and shortest path problems inside triangulated simple polygons. *Algorithmica*,
 648 2(1-4):209–233, 1987.
- 649 11 L. J. Guibas and J. Hershberger. Optimal shortest path queries in a simple polygon. In
 650 *Proceedings of STOC*, pages 50–63. ACM, 1987.
- 651 12 D. Harel and R. E. Tarjan. Fast algorithms for finding nearest common ancestors. *SIAM*
 652 *Journal on Computing*, 13(2):338–355, 1984.
- 653 13 J. Hershberger and S. Suri. Matrix searching with the shortest path metric. In *Proceedings*
 654 *of STOC*, pages 485–494. ACM, 1993.
- 655 14 Y. Ke. An efficient algorithm for link-distance problems. In *Proceedings of SoCG*, pages
 656 69–78, 1989.
- 657 15 D.-T. Lee and F. P. Preparata. Euclidean shortest paths in the presence of rectilinear
 658 barriers. *Networks*, 14(3):393–410, 1984.
- 659 16 J. Matoušek. Approximations and optimal geometric divide-and-conquer. In *Proceedings*
 660 *of STOC*, pages 505–511. ACM, 1991.
- 661 17 J. Matoušek. Construction of epsilon nets. In *Proceedings of SoCG*, pages 1–10, New York,
 662 1989. ACM.
- 663 18 N. Megiddo. On the ball spanned by balls. *Discrete & Computational Geometry*, 4(1):605–
 664 610, 1989.
- 665 19 J. S. B. Mitchell. Geometric shortest paths and network optimization. In J.-R. Sack and
 666 J. Urrutia, editors, *Handbook of Computational Geometry*, pages 633–701. Elsevier, 2000.

- 667 20 B. Nilsson and S. Schuierer. Computing the rectilinear link diameter of a polygon. In
668 *Proceedings of CG*, pages 203–215, 1991.
- 669 21 B. Nilsson and S. Schuierer. An optimal algorithm for the rectilinear link center of a
670 rectilinear polygon. *Computational Geometry: Theory and Applications*, 6:169–194, 1996.
- 671 22 R. Pollack, M. Sharir, and G. Rote. Computing the geodesic center of a simple polygon.
672 *Discrete & Computational Geometry*, 4(1):611–626, 1989.
- 673 23 S. Suri. *Minimum Link Paths in Polygons and Related Problems*. PhD thesis, Johns Hopkins
674 Univ., 1987.
- 675 24 S. Suri. Computing geodesic furthest neighbors in simple polygons. *Journal of Computer
676 and System Sciences*, 39(2):220–235, 1989.